

Article

Impact of Missense Mutations on Spike Protein Stability and Binding Affinity in the Omicron Variant

Vidhyanand Mahase ¹, Adebiyi Sobitan ¹, Qiaobin Yao ¹, Xinghua Shi ², Hong Qin ³, Dawit Kidane ⁴, Qiyi Tang ⁵ and Shaolei Teng ^{1,*}

- Department of Biology, Howard University, Washington, DC 20059, USA; vidhyanand.mahase@bison.howard.edu (V.M.); adebiyi.sobitan@bison.howard.edu (A.S.); qiaobin.yao@bison.howard.edu (Q.Y.)
- ² Department of Computer & Information Sciences, Temple University, Philadelphia, PA 19122, USA; mindyshi@temple.edu
- ³ Department of Computer Science and Engineering, University of Tennessee at Chattanooga, Chattanooga, TN 37403, USA; hong-qin@utc.edu
- ⁴ Department of Physiology and Biophysics, Howard University College of Medicine, Washington, DC 20059, USA; dawit.kidane-mulat@howard.edu
- Department of Microbiology, Howard University College of Medicine, Washington, DC 20059, USA; qiyi.tang@howard.edu
- * Correspondence: shaolei.teng@howard.edu

Abstract: The global effort to combat the COVID-19 pandemic faces ongoing uncertainty with the emergence of Variants of Concern featuring numerous mutations on the Spike (S) protein. In particular, the Omicron Variant is distinguished by 32 mutations, including 10 within its receptor-binding domain (RBD). These mutations significantly impact viral infectivity and the efficacy of vaccines and antibodies currently in use for therapeutic purposes. In our study, we employed structurebased computational saturation mutagenesis approaches to predict the effects of Omicron missense mutations on RBD stability and binding affinity, comparing them to the original Wuhan-Hu-1 strain. Our results predict that mutations such as G431W and P507W induce the most substantial destabilizations in the Wuhan-Hu-1-S/Omicron-S RBD. Notably, we postulate that mutations in the Omicron-S exhibit a higher percentage of enhancing binding affinity compared to Wuhan-S. We found that the mutations at residue positions G447, Y449, F456, F486, and S496 led to significant changes in binding affinity. In summary, our findings may shed light on the widespread prevalence of Omicron mutations in human populations. The Omicron mutations that potentially enhance their affinity for human receptors may facilitate increased viral binding and internalization in infected cells, thereby enhancing infectivity. This informs the development of new neutralizing antibodies capable of targeting Omicron's immune-evading mutations, potentially aiding in the ongoing battle against the COVID-19 pandemic.

Keywords: SARS-CoV-2; COVID-19; Spike protein; Omicron Variant; computational saturation mutagenesis

Citation: Mahase, V.; Sobitan, A.; Yao, Q.; Shi, X.; Qin, H.; Kidane, D.; Tang, Q.; Teng, S. Impact of Missense Mutations on Spike Protein Stability and Binding Affinity in the Omicron Variant. *Viruses* **2024**, *16*, x. https://doi.org/10.3390/xxxxx

Academic Editor(s): Name

Received: date Revised: date Accepted: date Published: date



Copyright: © 2024 by the authors. Submitted for possible open access publication under the terms and conditions of the Creative Commons Attribution (CC BY) license (https://creativecommons.org/license s/by/4.0/).

1. Background

In April 2022, the Omicron subvariants, specifically BA.4/BA.5, were identified and rapidly propagated around the globe. During early July 2022, these variants had grown to constitute nearly 80% of all COVID-19 cases in America [1]. As the virus undergoes continuous evolution and accumulates genetic changes, the Omicron variant has been classified as a Variant of Concern (VOC), contributing to a significant upsurge in new cases, surpassing 400,000 cases in the United States alone [2]. VOCs pose significant challenges due to their demonstrated increased transmissibility, severe disease manifestations, enhanced ability to evade diagnostic tests, and reduced neutralization by antibodies

from vaccinations. The Omicron variant has outpaced other VOCs, bearing a higher number of mutations, particularly in the Spike (S) protein [3]. Given the multitude of S protein mutations, it is possible that many of these missense mutations impact the S protein's stability and binding affinity to its human receptors. The computational saturation mutagenesis offers a rapid approach to predict the functional implications of mutations on protein stability and protein–protein interactions of coronavirus S proteins [4–6].

The S glycoprotein is the crucial protein that determines viral host selection and pathology, making it a target for both diagnostic and therapeutic interventions. The S₁ domain, responsible for receptor binding, is divided into an N-terminal domain (NTD: 14-305) and a receptor-binding domain (RBD: 319-541) [7]. Notably, the receptor-binding motif (RBM: 437–508) of the RBD directly interacts with the ACE2 receptor, highlighting the significance of this region in the infection process. A recent study identified 22 amino acid substitutions in the RBM of the Omicron variant, with specific positions (475-477, 489, 493, and 501) attributed to its heightened binding ability to the receptor [8]. The closely related BA.4 and BA.5 variants share lineage with the Omicron BA.2 variant, but exhibit unique mutations, including A484E, R498Q, and Y501N, in their amino acid sequences compared to their predecessor [9]. Notably, the Omicron variant surpasses previous variants with the highest number of mutations in the RBM, such as A484E and R493Q, associated with immune evasion by reducing bindings to host antibodies [10]. To gain a deeper understanding of the Omicron variant's impact on infection rates and its ability to evade immunity, it is crucial to unravel the molecular mechanisms governing its receptor-recognition capabilities [11].

SARS-CoV-2, in contrast to past seasonal coronaviruses and influenza A, demonstrates a markedly accelerated rate of evolution and propagation. Significantly, many monoclonal antibodies targeting the RBM have shown reduced efficacy in neutralizing the Omicron variant, although some antibodies continue to recognize Omicron through antigenic binding sites outside the RBM [12]. Analyzing the atomic-level structure of SARS-CoV-2 and its variants provides valuable insights into their interactions with susceptible cells during infection. This knowledge aids in identifying robust target regions for neutralizing antibodies, supporting the development of drugs and vaccines to combat SARS-CoV-2. In this study, we applied structure-based computational strategies to investigate all S mutations in Omicron and Wuhan-Hu-1 that affect protein stability ($\Delta\Delta$ G). Our results predict how the S RBM mutations might affect the binding affinity ($\Delta\Delta$ G) within both Omicron-S-ACE2 and Wuhan-Hu-1-S-ACE2 complexes. Our findings shed light on specific residues that warrant further experimental validation, which is essential for designing effective neutralizing peptides to address the potential immunogenicity of the SARS-CoV-2 Omicron Variant.

2. Materials and Methods

2.1. Structure Collection

To investigate the impacts of S RBD mutations on the protein stability and binding, we compared the Omicron-S (PDB ID: 7WBP)—a crystal structure of the RBD of Omicron variant S in complex with its receptor human ACE2—with the original strain Wuhan-Hu-1 S RBD–ACE 2 complex (PDB ID: 6LZG). Both structures were obtained from the Protein Data Bank [13]. Structural alignments and 3D structural images were generated using PyMol's 'fetch' and 'align' commands [14].

2.2. Free Energy Calculations

The FoldX [15] was employed to calculate the free energies, investigating the effects of RBD mutations on protein stability and binding affinity in both the Omicron S–ACE2 and Wuhan-Hu-1 S–ACE2 complexes. Prior to energy calculations, all protein structures were repaired using the 'RepairPDB' command. The FoldX was utilized to perform computational saturation mutagenesis, total energy calculations. van der Waals interactions,

hydrogen bonding, etc. To analyze the effects of mutations on proteins, a Perl script was executed to generate lists of systematic changes in each residue. These lists were used within FoldX software (2023) to model the impact of mutations on the S RBD protein and the RBD–ACE2 complex.

The change in free folding energy ($\Delta\Delta G$) representing the difference between the mutant and wild-type protein free energy was computed using the repaired structures. The "BuildModel" function of FoldX generated mutant models for each desired protein by calculating the free energy change (ΔG) between a wildtype structure and its mutated version. This difference in folding free energy ($\Delta\Delta G$), where negative values indicate increased stability and positive values denote destabilization, was used to assess the impact of mutations on the overall protein conformation. Computational saturation mutagenesis was performed on the S-RBD of both Wuhan-Hu-1 and Omicron strains. For free-folding calculations, the stability values between the mutant (MUT) and wild-type (WT) residues were computed as follows:

$$\Delta G \text{ (folding)} = G \text{ (folded)} - G \text{ (unfolded)}$$
 (1)

$$\Delta \Delta G$$
 (stability) = ΔG (folding) MUT – ΔG (folding) WT (2)

The 'AnalyseComplex' command calculated the free-folding energy change between the interactions (binding energy change). By disassembling each protein and evaluating their distinct energies, the $\Delta\Delta G$ (binding) was determined. This value was then subtracted from the energy of the entire protein complex to derive the change in binding-free energy ($\Delta\Delta\Delta G$) by subtracting it from the wild-type complex. The change in binding-free energy ($\Delta\Delta\Delta G$) between the mutant and wild-type structures is given by the following equations:

$$\Delta \Delta G \text{ (binding)} = \Delta G \text{ (folding: AB)} - \Delta G \text{ (folding: A)} - \Delta G \text{ (folding: B)}$$
(3)

$$\Delta\Delta\Delta G \text{ (binding)} = \Delta\Delta G \text{ (binding)} MUT - \Delta\Delta G \text{ (binding)} WT$$
(4)

The folding energy changes ($\Delta\Delta G$) were classified into the following five groups: large decrease in stability ($\Delta\Delta G > 2.5$ kcal/mol), moderate decrease ($0.5 < \Delta\Delta G \le 2.5$ kcal/mol), neutral ($-0.5 < \Delta\Delta G \le 0.5$ kcal/mol), moderate increase ($-0.5 \le \Delta\Delta G < -2.5$ kcal/mol), and large increase ($\Delta\Delta G < -2.5$ kcal/mol). In the energy calculations, binding energy values are often smaller in magnitude than stability values due to stronger interactions formed during binding and favorable enthalpic contributions outweighing entropic losses. Additionally, computational methods differ, with binding energy calculations focusing on the protein interface and stability calculations considering the entire protein, leading to variations in energy magnitudes. The binding energy changes ($\Delta\Delta\Delta G$) were categorized into the following five classifications: large decrease in binding affinity ($\Delta\Delta\Delta G > 0.5$ kcal/mol), moderate decrease ($0.1 < \Delta\Delta\Delta G \le 0.5$ kcal/mol), neutral ($-0.1 < \Delta\Delta\Delta G \le 0.1$ kcal/mol), moderate increase ($-0.5 \le \Delta\Delta\Delta G < -0.1$ kcal/mol), and large increase ($\Delta\Delta\Delta G < -0.5$ kcal/mol). The R package was used to generate heatmaps and line graphs for $\Delta\Delta G$ and $\Delta\Delta\Delta G$ values [16].

2.3. Sequence-Based Analysis

For sequence analysis, the S RBD amino acid sequences of Wuhan-Hu-1-S-ACE2 and Omicron-S-ACE2 were extracted from PDB (PDB ID: 6LZG and 7WBP). The full-length S sequence was obtained from Uniprot (ID: P0DTC2) [17]. A pairwise sequence alignment with an EMBOSS Needle (https://www.ebi.ac.uk/jdispatcher/psa/emboss_needle) was used to align the FASTA sequences of the Wuhan and Omicron spike proteins [18].

2.4. Mutation Collection

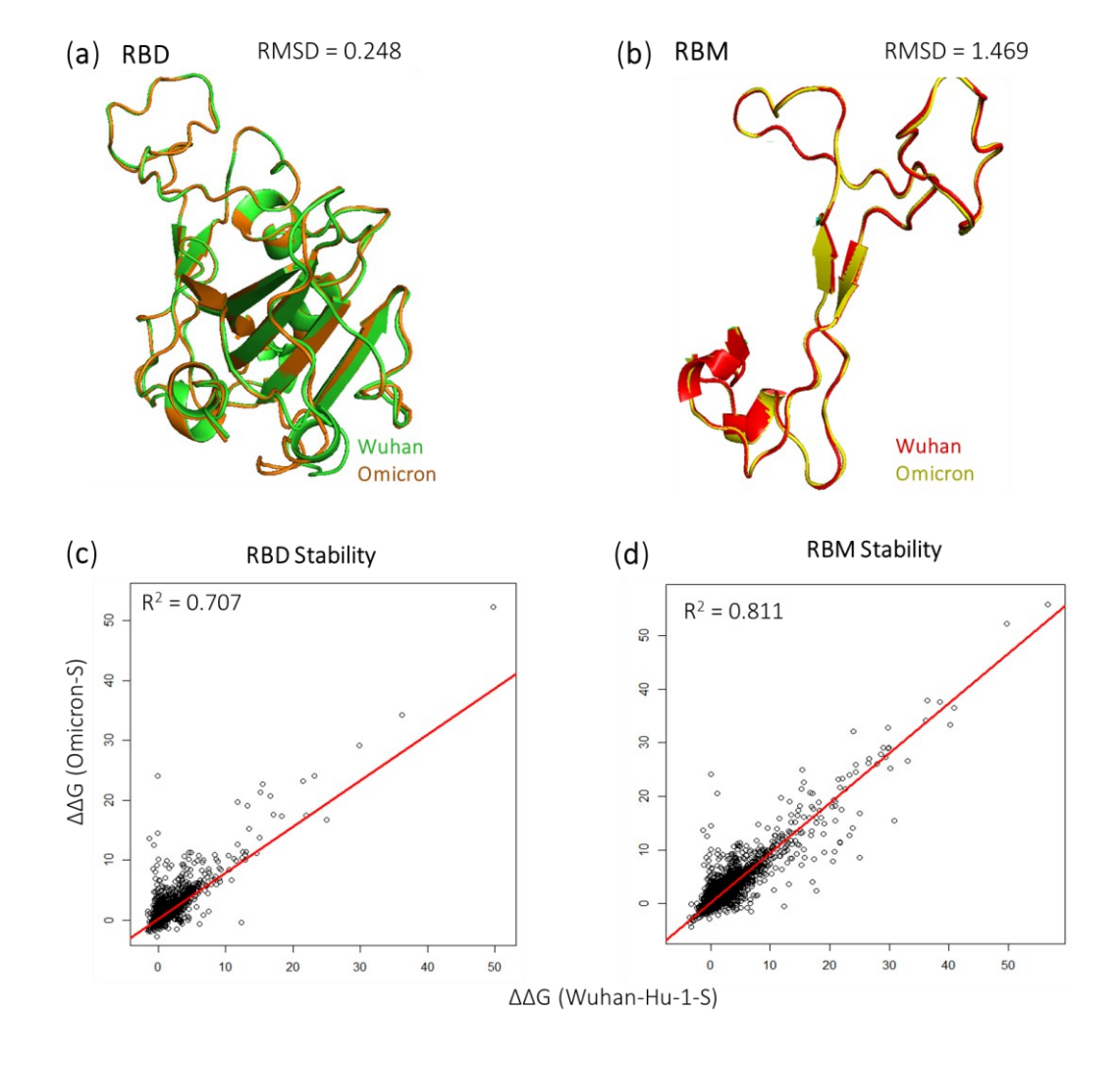
Omicron viral mutations were collected from the Stanford University Coronavirus Antiviral and Resistance Database (https://covdb.stanford.edu/) [19] and The National

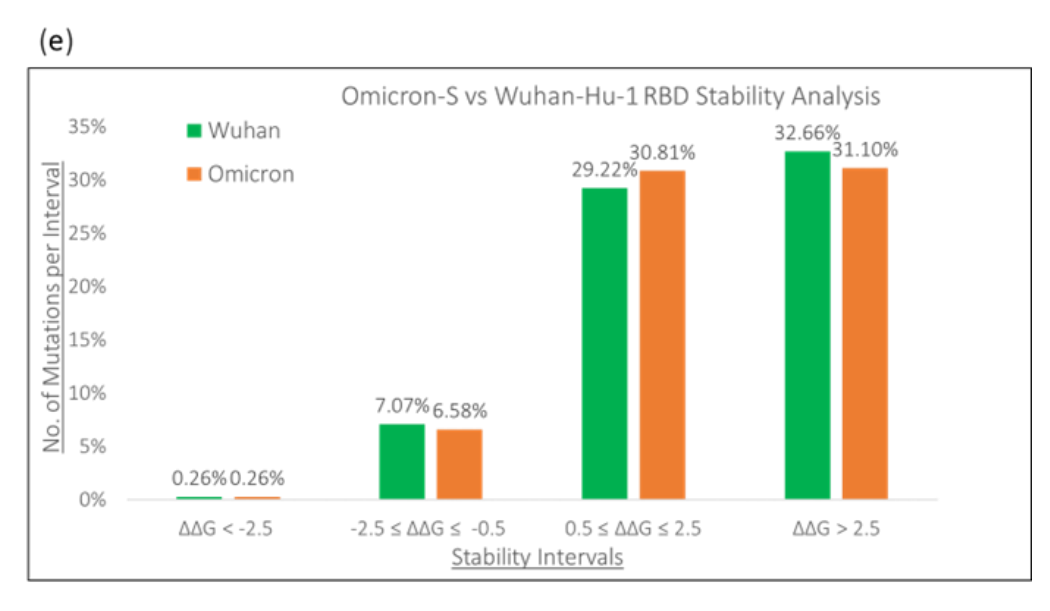
Genomics Data Center (NGDC), part of the China National Center for Bioinformation (CNCB) (https://ngdc.cncb.ac.cn/ncov/variation/annotation) [20].

3. Results

3.1. Effects of Omicron Mutations on Protein Stability

We performed structural alignment on the Wuhan-Hu-1-S and Omicron-S proteins in the Receptor-Binding Domain (RBD) and Receptor-Binding Motif (RBM) regions (Figure 1a,b). The root-mean-square deviation (RMSD) value indicates a high degree of similarity for the RBD = 0.248 over 195 residues, while the similarity is acceptable in the RBM with an RMSD = 1.469 over 72 residues. Our analysis extended to evaluating the folding energy changes ($\Delta\Delta G$) associated with all potential RBD and RBM mutations, aiming to estimate their impact on protein stability. Notably, the correlation analysis of $\Delta\Delta G$ demonstrated an r^2 value of 0.707 in RBD (Figure 1c), and 0.811 in the RBM (Figure 1d). This indicates that mutations in the RBM region may have a more consistent impact on protein stability compared to the RBD.





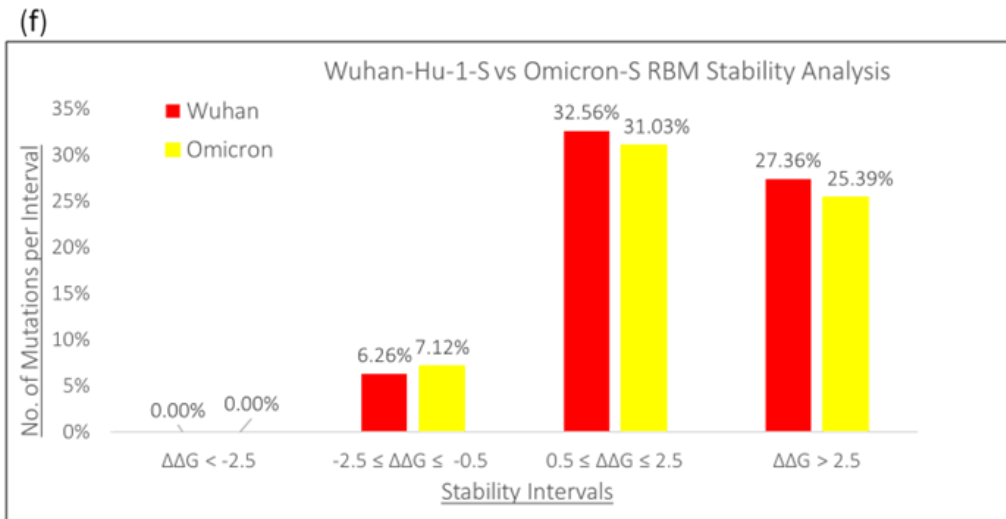


Figure 1. Structural alignment displaying the (a) RBD and (b) RBM of Wuhan-S/ Omicron-S proteins. The regression analysis shows $\Delta\Delta G$ values of RBD (c) and RBM (d) mutations of Wuhan-S/ Omicron-S proteins. Bar charts depictinWuhan-S/Omicron-S proteins distribution effects of mutations affecting RBD (e) and RBM (f) stability.

The folding energy changes ($\Delta\Delta G$) were classified as highly stabilizing ($\Delta\Delta G < -2.5$ kcal/mol), moderately stabilizing ($-2.5 \le \Delta\Delta G < -0.5$ kcal/mol), moderately destabilizing ($0.5 < \Delta\Delta G \le 2.5$ kcal/mol), and highly destabilizing ($\Delta\Delta G > 2.5$ kcal/mol). In the RBD, our analysis involved 3861 mutations for Wuhan-Hu-1-S and 3934 mutations for Omicron-S (Figure 1e). For highly stabilizing mutations, both S proteins were similar (0.26%). The Wuhan-Hu-1-S was greater in the moderately stabilizing (7.07%) and the highly destabilizing intervals (32.66%). However, the Omicron-S (30.81%) was greater in the moderately stabilizing category than the Wuhan-Hu-1-S (29.22%). Moving to the RBM, we analyzed 1417 mutations from the Omicron-S and 1422 mutations from the Wuhan-S. No highly stabilizing mutations were reported in the RBM for both complexes. As shown in Figure 1f, the Omicron-S displayed a more moderate stabilizing effect (7.12%) versus the Wuhan-S (6.26%). Conversely, the Wuhan-Hu-1-S displayed a higher percentage in both moderately destabilizing (32.56%) and highly destabilizing (27.36%) mutations.

3.2. Key Residues Predicted to Affect the RBD Stability of Omicron

In Figure 2, we illustrated line charts displaying the mean $\Delta\Delta G$ values for each residue position of the spike RBD proteins, as well as the corresponding $\Delta\Delta G$ values for alanine substitutions. Within the Omicron S-protein, the mutations in residue G431 showed the most significant destabilizing effects (mean $\Delta\Delta G$ = 24.65 kcal/mol), whereas the mutations in S514 exhibited the highest stabilizing effects (mean $\Delta\Delta G$ = -1.39 kcal/mol). A similar trend was observed in the Wuhan S-protein, with $\Delta\Delta G$ values ranging from 25.18 kcal/mol at G431 to -1.37 kcal/mol at S514. Heatmaps highlighting the residues with the greatest destabilizing and stabilizing effects on RBD protein stability, along with structural representations of these key residues, are also presented in Figure 2.

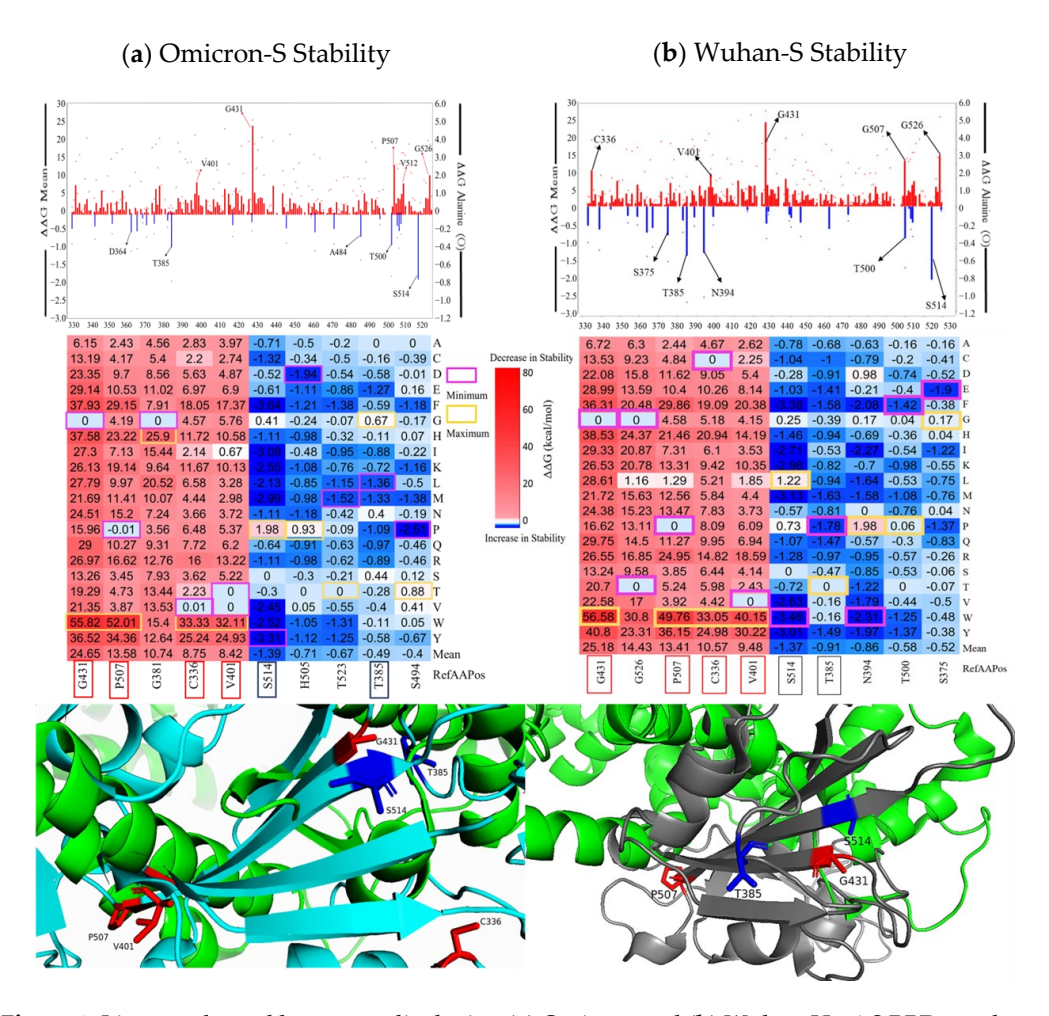


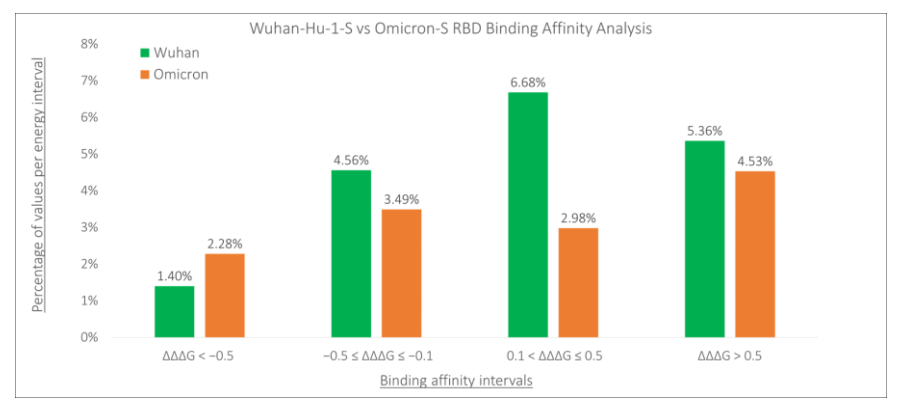
Figure 2. Line graphs and heatmaps displaying (a) Omicron and (b) Wuhan-Hu-1 S RBD top destabilizing/stabilizing values. Omicron-S is displayed in cyan, while the Wuhan-Hu-1-S is gray. ACE2 is depicted as green. The red squares indicate common destabilizing residues and positions in both heatmaps, while the blue squares indicate common stabilizing residues and positions in both heatmaps. The minimum energy values are in magenta, and the maximum energy values are in yellow.

Our study predicts that G431W and P507W are the most destabilizing mutations common to both RBD proteins. The G431W mutation resulted in substantial decreases in stability for both Omicron S and Wuhan-Hu-1 S proteins (56.58 kcal/mol and 55.82 kcal/mol, respectively). This destabilization is due to the substitution of glycine (G), which disrupts the heterotrimers, impairs helix formation, and reduces the molecule's overall stability. Moreover, it significantly diminishes interactions between extracellular molecules [21]. The P507W mutation (52.01 kcal/mol for Omicron-S and 49.76 kcal/mol for

Wuhan-Hu-1) is particularly destabilizing when proline (P) is located internally in α -helices or β -sheets [22]. In contrast, tryptophan (W) promotes structural hydrophobic interactions among proteins, peptides, and biomolecules [23]. The presence of tryptophan-R groups within transmembrane domains is essential for maintaining the structural integrity of membrane-bound proteins.

3.3. Effects of Omicron-S and Wuhan-Hu-1-S Mutations on Binding Affinity

We investigated the potential differences in the effects of mutations on protein binding affinity within the binding regions of Wuhan-Hu-1-S and Omicron-S proteins. Our analysis involved assessing the binding energy changes ($\Delta\Delta\Delta G$) of mutations and grouping the percentages of mutations based on specific intervals of $\Delta\Delta\Delta G$ values (Figure 3). In the RBD region, we evaluated 3860 mutations for Wuhan-Hu-1-S and 3727 mutations for Omicron-S. As shown in Figure 3A, Omicron-S showed a higher percentage (2.28%) compared to Wuhan-S (1.40%) (p-value = 1.26×10^{-5}) for mutations displaying a high increase in binding affinity ($\Delta\Delta\Delta G < -0.5$ kcal/mol). However, for moderate increases in binding affinity ($-0.5 \le \Delta\Delta\Delta G \le -0.1$ kcal/mol), Omicron-S exhibited a slightly lower percentage (3.49%) compared to Wuhan-S (4.56%) (p-value = 0.466). Regarding mutations with moderate decreases in binding affinity (0.1 < $\Delta\Delta\Delta G \le 0.5$ kcal/mol), Omicron-S also showed a lower percentage (2.98%) compared to Wuhan-S (6.68%) (p-value = 1.02 × 10⁻²⁹). The impact of Omicron-S on a significant increase in binding affinity ($\Delta\Delta\Delta G > 0.5$ kcal/mol) was also lower at 4.53% compared to 5.36% in Wuhan-S. In the RBM region, we analyzed 1411 mutations for Wuhan-Hu-1-S and 1355 mutations for Omicron-S. Interestingly, we observed that mutations in the Omicron-S displayed a higher percentage in stabilizing effects for protein complexes compared to Wuhan-S (Figure 3B). Notably, 6.35% of Omicron-S RBM mutations exhibited a significant increase in binding affinity ($\Delta\Delta\Delta G < -0.5$ kcal/mol), surpassing the 3.54% observed in Wuhan-Hu-1-S RBM mutations (p-value = 6.867 × 10⁻⁶). Additionally, 12.92% of Omicron-S mutations displayed a moderate increase in binding affinity ($-0.5 \le \Delta\Delta\Delta G \le -0.1$ kcal/mol), compared to 7.80% of Wuhan-S mutations (p-value = 1.24×10^{-5}). Conversely, Omicron-S showed a lower percentage (5.68%) compared to Wuhan-S (11.20%) for mutations exhibiting a moderate decrease in binding affinity. Furthermore, the Omicron-S variant showed a lower impact on a significant decrease in binding affinity ($\Delta\Delta\Delta G > 0.5$ kcal/mol), with a rate of 12.32% compared to 13.96% in the Wuhan-Hu-1-S variant.



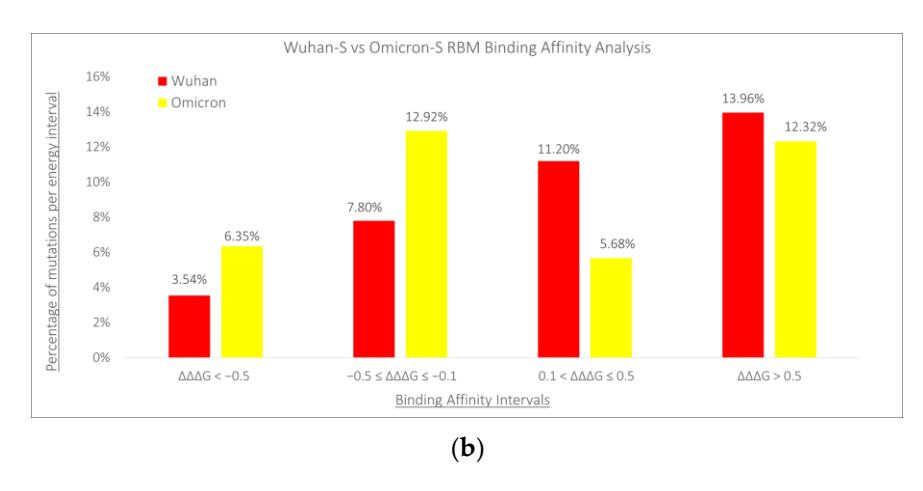


Figure 3. Bar charts displaying Wuhan-Hu-1-S vs Omicron-S binding affinity values ($\Delta\Delta\Delta G$) per energy interval in the RBD (**a**) and RBM (**b**) regions.

3.4. Key Sites Predicted to Alter the Omicron S RBD-ACE2 Binding Affinity

The mean $\Delta\Delta\Delta G$ values for each residue position of the spike RBD and RBM regions are shown in Figure 4. Notably, mutations at residues G502, F486, and F456 significantly reduce the binding affinity of both Omicron-S and Wuhan-Hu-1-S complexes. The mutations in G502 exhibit the most destabilizing effects for the Omicron S RBD–ACE2 complex (mean $\Delta\Delta\Delta G$ = 2.35 kcal/mol). Particularly noteworthy is the G502P mutation, which exerts the maximum destabilizing effect ($\Delta\Delta\Delta G$ = 11.97 kcal/mol) among all mutations analyzed.

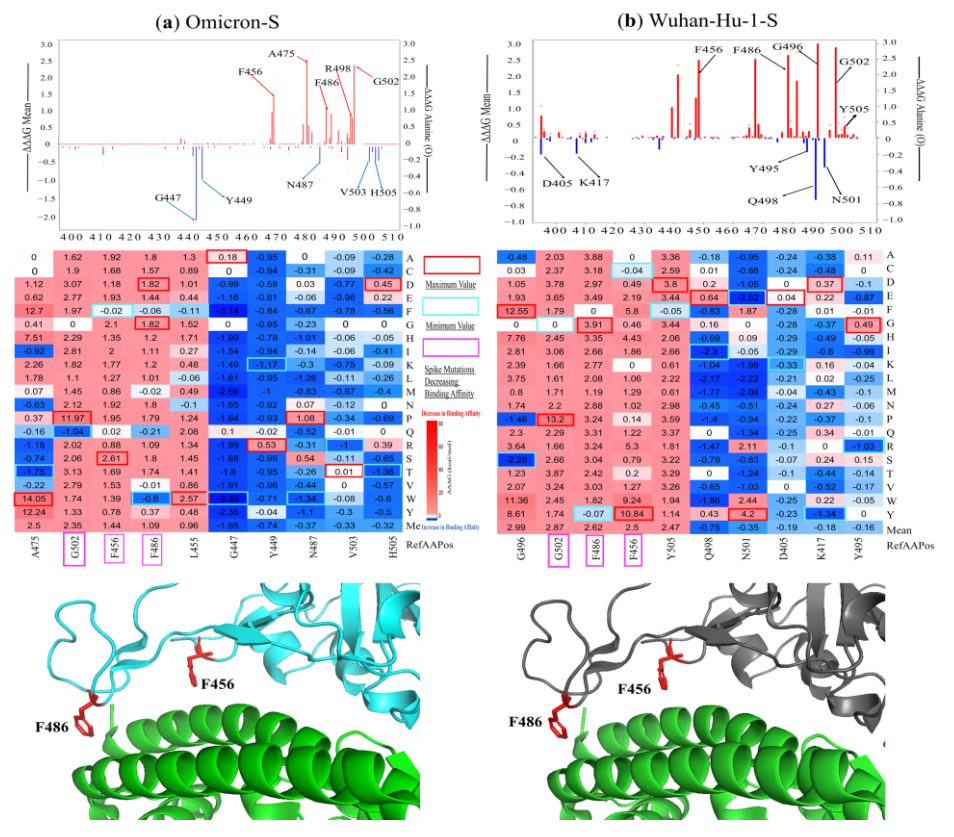


Figure 4. Key Spike positions and residues in ACE2-Omicron-S (a) and ACE2-Wuhan-HU-1-S (b) complexes. ACE2 is shown in green, the Wuhan-Hu-1-S is gray, and the Omicron-S is cyan. PyMol visuals show mutations causing an increase in binding affinity, which are shown in red. The heatmaps of key spike mutations, maximum values (red), minimum (cyan), and mutations decreasing binding affinity (fuchsia) are also indicated.

3.5. Predicted Changes in Binding Affinity of Omicron-S and Wuhan-Hu-1-S

We observed the distinct effects of mutations on predicted binding affinity in certain positions of Omicron-S compared to the Wuhan-Hu-1-S (Figure 5). Notably, some mutations at certain positions of Omicron-S, including Y449, G447, and 496, can stabilize the Omicron-S RBD-ACE2 complex, but destabilized the Wuhan-Hu-1-S RBD-ACE2 complex. Mutations in residues F456 and F486 significantly reduce the binding affinity of the Wuhan-Hu-1-S RBD-ACE2 complex. Located in the ACE2-RBD interface, F456 and F486 interact with ACE2 residues 19 to 42, altering the electrostatic surface charges at the interface. This process can also affect antibody-drug binding due to the larger size of the mutated side chains [24].

Specifically, the F456A ($\Delta\Delta\Delta G$ mean = 3.36 kcal/mol in Wuhan-Hu-1-S, and 1.92 kcal/mol in Omicron-S) is a class 1 epitope that generally weakened immunization levels by vaccine sera, though it has a limited effect on convalescent sera [25]. Moreover, this mutation is not found in native sequences, and significantly decreases viral entry titers. The F456 of the Omicron variant formed a strong hydrogen bond with Q24 and T27 found in ACE2, whereas this bond is lacking in other VOCs [11]. Another example is the F486V mutation, which has a $\Delta\Delta\Delta G$ of 3.03 kcal/mol in Wuhan-Hu-1-S and -0.01 kcal/mol in Omicron-S. This mutation has been analyzed through deep mutational scanning of the SARS-CoV-2 receptor binding domain. Researchers suggest that the mutation at residue F486 in Omicron BA.1/2 could lead to further evasion from antibodies found in individuals who experienced pre-Omicron and Omicron BA.1 infection. Interestingly, F486V variants have been identified among lineages of Omicron BA.4/5, contributing to a fifth epidemic wave sweeping across South Africa [26].

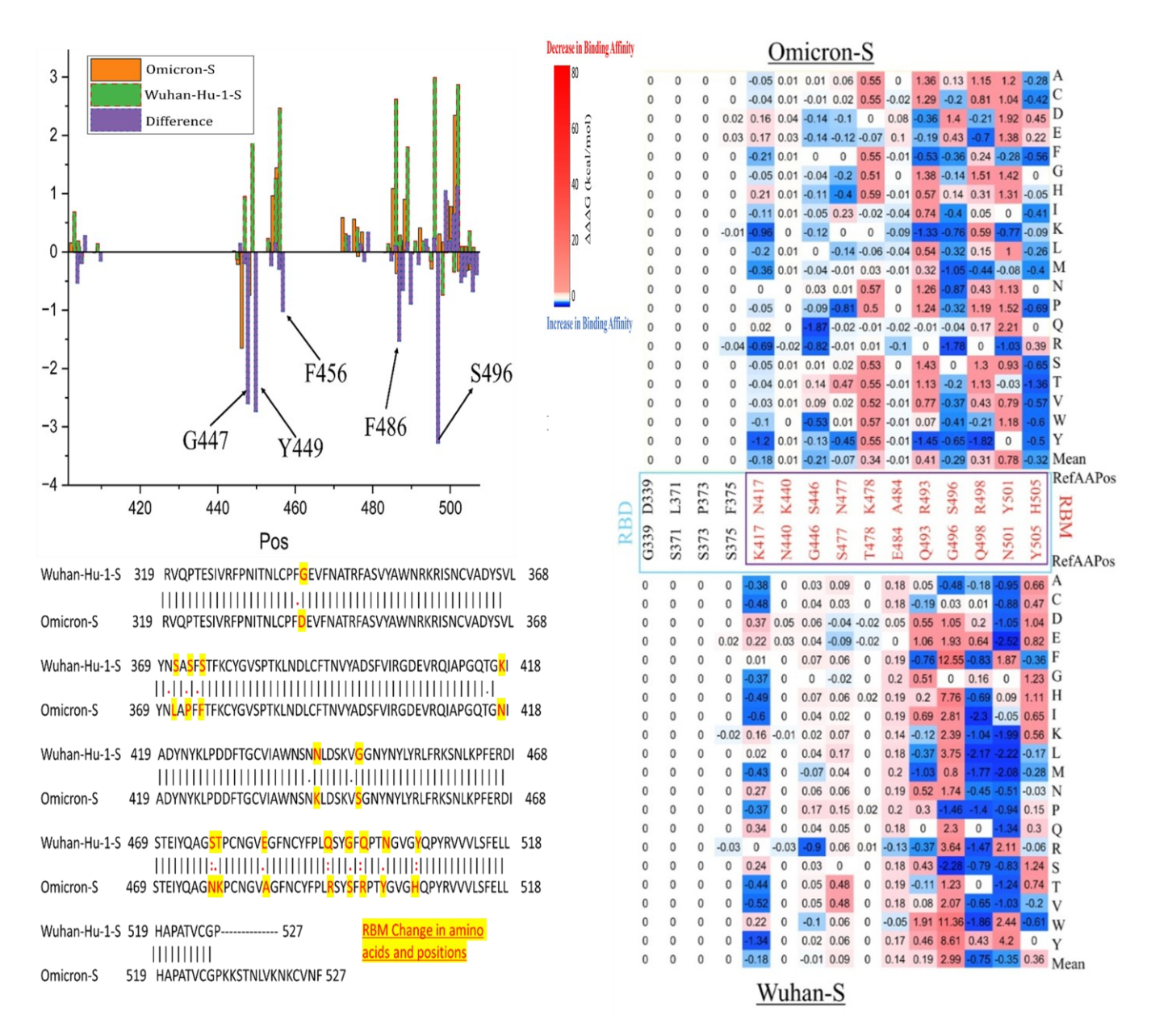


Figure 5. Changes in binding affinity of Omicron-S-ACE2 and Wuhan-Hu-1-S-ACE2 complexes.

4. Discussion

4.1. Differences between Omicron Variants vs. Alpha, Beta, Gamma, and Delta

The Omicron RBM harbors mutations that confer increased transmissibility and infectivity of SARS-CoV-2-S compared to previous variants like alpha, beta, gamma, and delta (Table 1). The heatmaps depicting key residues in the RBM are presented in Figure 5. Most of these mutations are located in the S protein, which allows it to fit securely into the ACE2 receptor, much like a precisely crafted key into a lock [24]. This facilitates easier access for virions to host cells, resulting in greater transmissibility among people. It is hypothesized that the rapid mutation rate leading to the emergence of the Omicron variant may be due to its prolonged persistence in immunocompromised individuals, such as those with HIV/AIDS. Regions with high HIV infection rates, like Southern Africa, are suggested as potential origins for this strain [1]. Amino acid substitutions in the RBM contribute to greater escape from immune responses initiated by vaccines developed for preceding variants. Notable amino acid changes include Q498R and F486V (Table 1). As a result, Omicron has increased resistance to both vaccines and previous variants of the

virus, leading to increased virulence. Unlike the alpha and delta variants, which are associated with severe illness and high fatality rates alongside high transmissibility, the Omicron variant displays lower lethality, but exhibits an exceptionally rapid transmission rate. Evolutionary analyses indicate that Omicron likely diverged neither from neither alpha, beta, gamma, nor delta variants, further highlighting its unique evolutionary trajectory [27]. As shown in Figure 5, our computational evidence predicts changes in binding affinity for specific missense mutations, such as Q498R ($\Delta\Delta\Delta G = -1.47$ kcal/mol in Wuhan-Hu-1-S). Numerous studies indicate that the Omicron variant is significantly more infectious than its ancestral variant and other variants like beta and delta, primarily due to its extensive mutations in the RBM region [28]. Furthermore, two newly identified sub-lineages within Omicron, BA.4 and BA.5, exhibit even higher resistance to a wide range of monoclonal antibodies compared to the earlier BA.1 and BA.2 strains, suggesting an unprecedented level of infectivity for these viral mutations [29].

Table 1.	New	Omicron	RBD	mutations.

Synonyms	Lineages	Origin	RBM Mutations
Alpha	B.1.1.7	United Kingdom, October 2020	E484A, N501Y
Beta	B.1.351	E. Cape, South Africa, October 2020	K417N, E484K, N501Y
Gamma	P.1	Manaus, Brazil, March 2020	K417N/T, E484K, N501Y
Delta	B.1.617.2	Maharashtra, India, April 2020	L452R, K478T
Omicron	BA.4, BA.5	South Africa, January 2022	L452R, F486V
			D405N, R408S, K417N, N440K, K444T, G446S,
Omicron	BQ.1.1	United Kingdom, November 2022	L452R, N460K, S477N, T478K, E484A, F486V,
			Q498R, N501Y, Y505H
			D405N, R408S, K417N, N440K, K444T, V445P,
Omicron	XBB.1.5	United States, October 2022	G446S, N460K, S477N, T478K, E484A, F486V,
			F490S, Q498R, N501Y, Y505H

4.2. The RBM Is More Divergent Than the RBD in Omicron

Research indicates that the RBD, particularly the immunodominant RBM, exhibits high variability, enabling the virus to evade detection by the antibody response. Several studies have demonstrated that SARS-CoV-2 has a low genetic barrier to developing resistance to neutralizing antibodies targeting the RBD region [30]. This is due to the emergence of several independent mutations in the RBD region of the vesicular stomatitis virus SARS-CoV-2 chimeric system when exposed to antibody pressure. Hence, it is vital to monitor mutations in the RBD region, as they could significantly affect the progress of COVID-19 and its treatment options [31]. The RBM charge within the flexible loop region might have been altered by mutations, making it easier for binding to occur. The K417N, E484K, E484Q, and F490S, all known to aid antibody evasion, have minimal effects on ACE2 binding affinity, indicating no loss of fitness [32]. Regarding RBM-ACE2 binding affinity, interfaces between RBM and ACE2 show a significant increase in hydrogen bonds, indicating specific interactions between the two proteins. The shared residue, differing between SARS-CoV-2 and SARS-CoV, interacts with the same set of amino acids in ACE2, suggesting a comparable level of affinity for ACE2 between the two viruses. A key distinction in complex structures lies in the location of K417 in Wuhan-Hu-1-S, which, although outside the RBM, forms salt-bridge interactions with the D30 of ACE2. In contrast, the equivalent position in SARS-CoV-1 contains a valine residue, unable to form similar salt bridges. This slight difference may account for the slightly greater affinity between Wuhan-Hu-1-S RBD and ACE2 compared to SARS-CoV-1 [33]. In our analysis, the K417N mutation is observed to enhance the binding affinity ($\Delta\Delta\Delta G = -0.9231 \text{ kcal/mol}$), suggesting its potential impact on the virus's behavior and interaction with host cells.

4.3. Residue Changes G431W and P507W May Cause the Highest Destabilizations in Wuhan-Hu-1-S/Omicron-S RBM and RBD

Among all of the mutations present in Omicron-S, the glycine mutation G431W seems to cause the highest increase in positive folding energy with a value of $\Delta\Delta G$ = 55.82 kcal/mol. The mutations in glycine residue G431 have the most significant destabilizing effects on the RBD of the S-protein (mean $\Delta\Delta G = 24.65$ kcal/mol). When glycine (G), the smallest amino acid, is substituted with larger amino acids, it triggers unfavorable conformational changes, leading to protein instability [34]. Similarly, the mutation P507W seems to cause the second-highest destabilization ($\Delta\Delta G$ value = 52.01 kcal/mol). Proline has a unique side chain that loops back and reattaches to the parent amino group, which is different from other amino acids. Due to this structure, proline lacks a hydrogen atom on its nitrogen when it is part of a polypeptide chain. In contrast, tryptophan (W), characterized by the highest relative mutability among mutant residues, features an indole ring bound by a methylene group in its side chain. This structural configuration contributes to its substantial size and hydrophobic properties, further amplifying its destabilization effects [21]. These mutations might give the virus an advantage in evading detection by the immune system and increasing its contagiousness, likely by inducing specific structural modifications. Most of the sequence variations reported in the Omicron Variant are single nucleotide polymorphisms, which have resulted in an 85% reduction in the efficacy of neutralizing antibodies [35]. Viruses continually evolve, giving rise to new variants, some of which may possess characteristics that promote wider transmission or increased severity. However, the sheer number of infected individuals and the diverse array of potential targets raises concerns that new variants could undermine both vaccines and therapeutic interventions.

5. Conclusions

The S protein plays a pivotal role in viral infectivity, with mutations in its sequence present in all strains of interest or concern. Our research highlights the mutations G431W and P507W as possibly exhibiting the highest destabilizing effects in both Wuhan-Hu-1-S and Omicron-S. The emergence of various viral variants has led to increased infectivity and transmission rates, possibly driven by their enhanced affinity for the ACE2 receptor. We predict that mutations in Omicron-S display a higher tendency to enhance their binding affinity compared to Wuhan-Hu-1-S. Understanding the interaction between the RBD/RBM and ACE2 is essential not only for comprehending the behavior of different virus strains, but also for designing the effective therapeutic neutralizing antibodies. This knowledge can guide the development of the next generation of neutralizing antibodies capable of counteracting the immune-evading mechanisms of future SARS-CoV-2 variants.

Author Contributions: Conceptualization, Q.T. and S.T.; methodology, V.M., A.S., and S.T.; data curation, V.M., A.S., and Q.Y.; formal analysis, V.M.; data writing—original draft preparation, V.M. and S.T.; investigation, V.M., X.S., H.Q., D.K., Q.T., and S.T.; writing—review and editing, V.M., Q.Y., X.S., H.Q., D.K., Q.T., and S.T.; supervision, S.T.; funding acquisition, S.T. All authors have read and agreed to the published version of the manuscript.

Funding: This study received support from the National Science Foundation (DBI 2000296) and partially from the National Science Foundation (IIS 1924092 and HRD 2011933), as well as the National Institute on Minority Health and Health Disparities of the National Institutes of Health (2U54MD007597). The content is solely the responsibility of the author and does not represent the official views of the National Science Foundation and the National Institutes of Health. H.Q. thanks the support of the National Science Foundation 2200138.

Institutional Review Board Statement: Not applicable.

Informed Consent Statement: Not applicable.

Data Availability Statement: The original contributions presented in the study are included in the article, further inquiries can be directed to the corresponding authors.

Conflicts of Interest: The authors declare no competing interests.

References

- 1. Viana, R.; Moyo, S.; Amoako, D.G.; Tegally, H.; Scheepers, C.; Althaus, C.L.; Anyaneji, U.J.; Bester, P.A.; Boni, M.F.; Chand, M.; et al. Rapid Epidemic Expansion of the Sars-CoV-2 Omicron Variant in Southern Africa. *Nature* **2022**, *603*, *679*–*686*.
- 2. Al Rifai, M.; Jain, V.; Khan, S.U.; Nasir, K.; Zhu, D.; Vasudeva, R.; Lavie, C.J.; Dodani, S.; Petersen, L.A.; Virani, S.S. Social Vulnerability and COVID-19: An Analysis of Cdc Data. *Prog. Cardiovasc. Dis.* **2022**, *73*, 91–93.
- 3. Nikolaidis, M.; Papakyriakou, A.; Chlichlia, K.; Markoulatos, P.; Oliver, S.G.; Amoutzias, G.D. Comparative Analysis of Sars-CoV-2 Variants of Concern, Including Omicron, Highlights Their Common and Distinctive Amino Acid Substitution Patterns, Especially at the Spike Orf. *Viruses* **2022**, *14*, 707.
- 4. Sobitan, A.; Mahase, V.; Rhoades, R.; Williams, D.; Liu, D.; Xie, Y.; Li, L.; Tang, Q.; Teng, S. Computational Saturation Mutagenesis of Sars-Cov-1 Spike Glycoprotein: Stability, Binding Affinity, and Comparison with Sars-CoV-2. *Front. Mol. Biosci.* **2021**, *8*, 784303.
- 5. Teng, S.; Sobitan, A.; Rhoades, R.; Liu, D.; Tang, Q. Systemic Effects of Missense Mutations on Sars-CoV-2 Spike Glycoprotein Stability and Receptor-Binding Affinity. *Brief. Bioinform.* **2021**, 22, 1239–1253.
- 6. Rhoades, R.; Sobitan, A.; Mahase, V.; Gebremedhin, B.; Tang, Q.; Rawat, D.; Cao, H.; Teng, S. In-Silico Investigation of Systematic Missense Mutations of Middle East Respiratory Coronavirus Spike Protein. *Front. Mol. Biosci.* **2022**, *9*, 933553.
- 7. Mittal, A.; Manjunath, K.; Ranjan, R.K.; Kaushik, S.; Kumar, S.; Verma, V. Covid-19 Pandemic: Insights into Structure, Function, and Hace2 Receptor Recognition by Sars-CoV-2. *PLoS Pathog.* **2020**, *16*, e1008762.
- 8. Kumar, R.; Murugan, N.A.; Srivastava, V. Improved Binding Affinity of Omicron's Spike Protein for the Human Angiotensin-Converting Enzyme 2 Receptor Is the Key Behind Its Increased Virulence. *Int. J. Mol. Sci.* **2022**, *23*, 3409.
- 9. Tegally, H.; Moir, M.; Everatt, J.; Giovanetti, M.; Scheepers, C.; Wilkinson, E.; Subramoney, K.; Makatini, Z.; Moyo, S.; Amoako, D.G.; et al. Emergence of Sars-CoV-2 Omicron Lineages Ba.4 and Ba.5 in South Africa. *Nat. Med.* **2022**, *28*, 1785–1790.
- 10. Starr, T.N.; Greaney, A.J.; Addetia, A.; Hannon, W.W.; Choudhary, M.C.; Dingens, A.S.; Li, J.Z.; Bloom, J.D. Prospective Mapping of Viral Mutations That Escape Antibodies Used to Treat COVID-19. *Science* **2021**, *371*, 850–854.
- 11. Hachmann, N.P.; Miller, J.; Collier, A.Y.; Ventura, J.D.; Yu, J.; Rowe, M.; Bondzie, E.A.; Powers, O.; Surve, N.; Hall, K.; et al. Neutralization Escape by Sars-CoV-2 Omicron Subvariants Ba.2.12.1, Ba.4, and Ba.5. N. Engl. J. Med. 2022, 387, 86–88.
- 12. Li, X.; Pan, Y.; Yin, Q.; Wang, Z.; Shan, S.; Zhang, L.; Yu, J.; Qu, Y.; Sun, L.; Gui, F.; et al. Structural Basis of a Two-Antibody Cocktail Exhibiting Highly Potent and Broadly Neutralizing Activities against Sars-CoV-2 Variants Including Diverse Omicron Sublineages. *Cell Discov.* **2022**, *8*, 87.
- 13. Burley, S.K.; Berman, H.M.; Duarte, J.M.; Feng, Z.; Flatt, J.W.; Hudson, B.P.; Lowe, R.; Peisach, E.; Piehl, D.W.; Rose, Y.; et al. Protein Data Bank: A Comprehensive Review of 3d Structure Holdings and Worldwide Utilization by Researchers, Educators, and Students. *Biomolecules* **2022**, *12*, 1425.
- 14. Rigsby, R.E.; Parker, A.B. Using the Pymol Application to Reinforce Visual Understanding of Protein Structure. *Biochem. Mol. Biol. Educ.* **2016**, *44*, 433–437.
- 15. Delgado, J.; Radusky, L.G.; Cianferoni, D.; Serrano, L. Foldx 5.0: Working with Rna, Small Molecules and a New Graphical Interface. *Bioinformatics* **2019**, *35*, 4168–4169.
- 16. Gu, Z.; and Hubschmann, D. Make Interactive Complex Heatmaps in R. Bioinformatics 2022, 38, 1460-1462.
- 17. Wu, C.H.; Apweiler, R.; Bairoch, A.; Natale, D.A.; Barker, W.C.; Boeckmann, B.; Ferro, S.; Gasteiger, E.; Huang, H.; Lopez, R.; et al. The Universal Protein Resource (Uniprot): An Expanding Universe of Protein Information. *Nucleic Acids Res.* **2006**, 34, D187–D191.
- 18. Madeira, F.; Pearce, M.; Tivey, A.R.N.; Basutkar, P.; Lee, J.; Edbali, O.; Madhusoodanan, N.; Kolesnikov, A.; Lopez, R. Search and Sequence Analysis Tools Services from Embl-Ebi in 2022. *Nucleic Acids Res.* **2022**, *50*, W276–W279.
- 19. Tzou, P.L.; Tao, K.; Pond, S.L.K.; Shafer, R.W. Coronavirus Resistance Database (Cov-Rdb): Sars-CoV-2 Susceptibility to Monoclonal Antibodies, Convalescent Plasma, and Plasma from Vaccinated Persons. *PLoS ONE* **2022**, *17*, e0261045.
- 20. Yang, X.; Tang, B.; Pan, Y.H.; Yang, J.; Duan, G.; Zhu, J.; Hao, Z.Q.; Mu, H.; Dai, L.; et al. Coronavirus Genbrowser for Monitoring the Transmission and Evolution of Sars-CoV-2. *Brief. Bioinform.* **2022**, 23, bbab583.
- 21. Salacinska, K.; Michalus, I.; Pinkier, I.; Rutkowska, L.; Chlebna-Sokol, D.; Jakubowska-Pietkiewicz, E.; Kepczynski, L.; Salachna, D.; Gach, A. The First Glycine-to-Tryptophan Substitution in the Col1a1 Gene Identified in a Patient with Progressively-Deforming Osteogenesis Imperfecta. *Mol. Genet. Genomic Med.* **2022**, *10*, e1996.
- 22. Yu, H.; Zhao, Y.; Guo, C.; Gan, Y.; Huang, H. The Role of Proline Substitutions within Flexible Regions on Thermostability of Luciferase. *Biochim. Biophys. Acta* **2015**, *1854*, 65–72.
- 23. de Jesus, A.J.; Allen, T.W. The Role of Tryptophan Side Chains in Membrane Protein Anchoring and Hydrophobic Mismatch. *Biochim. Biophys. Acta* **2013**, *1828*, 864–876.
- 24. Lupala, C.S.; Ye, Y.; Chen, H.; Su, X.D.; Liu, H. Mutations on Rbd of Sars-CoV-2 Omicron Variant Result in Stronger Binding to Human Ace2 Receptor. *Biochem. Biophys. Res. Commun.* **2022**, 590, 34–41.

- 25. Greaney, A.J.; Loes, A.N.; Crawford, K.H.D.; Starr, T.N.; Malone, K.D.; Chu, H.Y.; Bloom, J.D. Comprehensive Mapping of Mutations in the Sars-CoV-2 Receptor-Binding Domain That Affect Recognition by Polyclonal Human Plasma Antibodies. *Cell Host Microbe* **2021**, 29, 463–476 e6.
- 26. Sun, K.; Tempia, S.; Kleynhans, J.; von Gottberg, A.; McMorrow, M.L.; Wolter, N.; Bhiman, J.N.; Moyes, J.; Carrim, M.; Martinson, N.A.; et al. Rapidly Shifting Immunologic Landscape and Severity of Sars-CoV-2 in the Omicron Era in South Africa. *Nat. Commun.* **2023**, *14*, 246.
- 27. Sun, Y.; Lin, W.; Dong, W.; Xu, J. Origin and Evolutionary Analysis of the Sars-CoV-2 Omicron Variant. *J. Biosaf. Biosecur.* **2022**, 4.33–37.
- 28. Araf, Y.; Akter, F.; Tang, Y.D.; Fatemi, R.; Parvez, M.S.A.; Zheng, C.; Hossain, M.G. Omicron Variant of Sars-CoV-2: Genomics, Transmissibility, and Responses to Current COVID-19 Vaccines. *J. Med. Virol.* **2022**, *94*, 1825–1832.
- 29. Cao, Y.; Yisimayi, A.; Jian, F.; Song, W.; Xiao, T.; Wang, L.; Du, S.; Wang, J.; Li, Q.; Chen, X.; et al. Ba.2.12.1, Ba.4 and Ba.5 Escape Antibodies Elicited by Omicron Infection. *Nature* **2022**, *608*, 593–602.
- 30. Alam, I.; Radovanovic, A.; Incitti, R.; Kamau, A.A.; Alarawi, M.; Azhar, E.I.; Gojobori, T. Covmt: An Interactive Sars-CoV-2 Mutation Tracker, with a Focus on Critical Variants. *Lancet Infect. Dis.* **2021**, 21, 602.
- 31. Tuekprakhon, A.; Nutalai, R.; Dijokaite-Guraliuc, A.; Zhou, D.; Ginn, H.M.; Selvaraj, M.; Liu, C.; Mentzer, A.J.; Supasa, P.; Duyvesteyn, H.M.E.; et al. Antibody Escape of Sars-CoV-2 Omicron Ba.4 and Ba.5 from Vaccine and Ba.1 Serum. *Cell* **2022**, *185*, 2422–2433 e13.
- 32. Gu, H.; Chen, Q.; Yang, G.; He, L.; Fan, H.; Deng, Y.Q.; Wang, Y.; Teng, Y.; Zhao, Z.; Cui, Y.; Li, Y.; et al. Adaptation of Sars-CoV-2 in Balb/C Mice for Testing Vaccine Efficacy. *Science* **2020**, *369*, 1603–1607.
- 33. Li, F. Structure, Function, and Evolution of Coronavirus Spike Proteins. Annu. Rev. Virol. 2016, 3, 237-261.
- 34. Nuytinck, L.; Tukel, T.; Kayserili, H.; Apak, M.Y.; De Paepe, A. Glycine to Tryptophan Substitution in Type I Collagen in a Patient with Oi Type Iii: A Unique Collagen Mutation. *J. Med. Genet.* **2000**, *37*, 371–375.
- 35. Cao, Y.; Wang, J.; Jian, F.; Xiao, T.; Song, W.; Yisimayi, A.; Huang, W.; Li, Q.; Wang, P.; An, R.; et al. Omicron Escapes the Majority of Existing Sars-CoV-2 Neutralizing Antibodies. *Nature* **2020**, *602*, 657–663.

Disclaimer/Publisher's Note: The statements, opinions and data contained in all publications are solely those of the individual author(s) and contributor(s) and not of MDPI and/or the editor(s). MDPI and/or the editor(s) disclaim responsibility for any injury to people or property resulting from any ideas, methods, instructions or products referred to in the content.